ISBN 9781740524094

Ultrasonic monitoring of compressive damage evolution in concrete

Aditya Khanna[1,a*], Andrei Kotousov[1,b], Ching-Tai Ng[2,c] and L.R. Francis Rose[3,d]

[1]School of Mechanical Engineering, The University of Adelaide, Adelaide, SA 5005, Australia

[2]School of Civil, Environmental and Mining Engineering, The University of Adelaide, Adelaide, SA 5005, Australia

[3] Aerospace Division, Defence Science & Technology Group, Melbourne, VIC 3207, Australia

[a]aditya.khanna@adelaide.edu.au, [b]andrei.kotousov@adelaide.edu.au
[c]alex.ng@adelaide.edu.au, [d]francis.rose@dst.defence.gov.au

Keywords: Concrete, Microcracking, Damage, Nonlinear ultrasonic inspection, Rayleigh waves.

Abstract. This paper presents the outcomes of an experimental study conducted on a short concrete column loaded to failure under uniaxial compression. Piezoceramic transducers bonded to the free surfaces of the specimen were used for ultrasonic inspection during the progressive loading. The evolution of damage was monitored by means of change in ultrasonic wave velocity and scaling subtraction method, with the aim to highlight the capabilities and limitations of these approaches. The results show that the change in the nonlinear parameter derived by the scaling subtraction method is over two orders of magnitude greater than the relative change in the Rayleigh wave speed, thereby indicating the much greater sensitivity of the nonlinear ultrasonics approach for damage detection.

Introduction

Over the past two decades, Non-Destructive Testing (NDT) techniques have gained prominence in the structural integrity management of concrete-based infrastructure assets across the world [1]. The usefulness of NDT techniques is strongly linked to the smallest defect size that can be reliably detected. This is because the time between the formation of a detectable defect and failure largely determines the frequency of safety inspections, and consequently, the maintenance costs [2]. This provides the motivation for the continuous improvement of defect detection techniques.

Linear ultrasonic techniques have been extensively utilised in NDT applications and rely on changes in wave velocity, phase or amplitude to locate and identify structural defects and measure the elastic properties of materials [3]. However, these techniques are only sensitive to defects or microstructural features which are comparable in size to the ultrasonic wavelength [4]. Frequencies less than 100 kHz are generally utilised for ultrasonic testing of concrete, since higher frequency waves experience significant attenuation and distortion in the heterogeneous medium [5].

Nonlinear ultrasonic techniques, such as higher harmonic generation, vibro-acoustic modulation and scaling subtraction method, are promising tools for early detection of damage, i.e. the detection of damage that cannot be resolved using linear ultrasonic techniques at typical testing frequencies. The latter techniques rely on measuring the nonlinear response of the propagating medium, which originates from the localised deformation of compliant features such as micro-cracks, voids and grain boundaries under applied stress [6]. The nonlinear response may manifest itself in a variety of ways, including resonance frequency shift, harmonic generation, frequency mixing, nonlinear attenuation and slow dynamic effects [6, 7]. The nonlinear response of concrete and other cement-based composite materials is strongly enhanced with the accumulation and propagation of micro-cracks (aperture of few microns) in the cement matrix and along the matrix/aggregate interfaces [8]. These features make nonlinear ultrasonic techniques suitable for early detection of distributed damage (micro-cracking), despite the wavelength being much larger than the defect size [7, 8].

In this paper, the sensitivity of some linear and nonlinear ultrasonic techniques to compressive damage in concrete specimens is investigated and compared. A similar comparative assessment was undertaken previously [9] and the key highlights of the present study are: (1) ultrasonic inspection with Rayleigh (surface) waves rather than Longitudinal (bulk) waves, and (2) the demonstration of the inspection technique on a test specimen with dimensions typical of realistic structural members.

Experimental setup

The experiments were conducted on a short concrete column with dimensions 300 × 300 × 600 mm. Piezoceramic disc transducers (Ferroperm Pz27) of diameter 10 mm and thickness 2 mm were bonded to the surface of the specimen using conductive epoxy glue and used for both excitation and sensing of the ultrasonic waves. Measurements were made for four actuator and sensor configurations described in Table 1, corresponding to four inspection zones along the front and back surfaces of the specimen. These inspection zones are shown in Fig. 1.

The transducer spacing, excitation frequency and pulse duration were selected empirically to ensure that the primary Rayleigh wave packet can be distinguished from bulk and surface waves reflected from the specimen boundaries. A 7-cycle Hann-windowed tone burst signal at 65 kHz was selected for the excitation of Rayleigh waves in the specimen. This excitation frequency is selected so that the wave reflections from the concrete aggregate are minimised [10]. The excitation signal was varied from 1.0 V_{pp} to 9.0 V_{pp} in 1 V increments and amplified by 20 dB using a Krohn-Hite 7602M amplifier. During the experiment, the transducers labelled F3 and B3 were used for excitation of Rayleigh waves in the front and back surfaces of the specimen, respectively. The sensor outputs were recorded using a National Instruments PXIe-5105 digital oscilloscope at a sampling frequency of 30 MHz and averaged 1000 times.

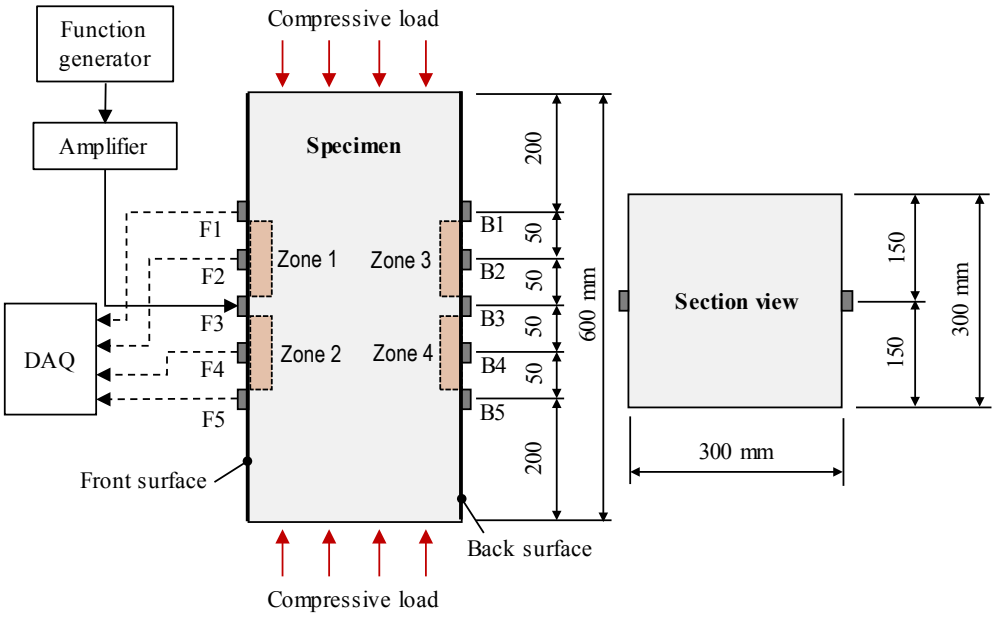

Fig. 1: Schematic diagram of the experimental setup showing transducer arrangement on the specimen.

Table 1: Actuator and sensor configurations for the four inspection zones on the specimen surface

Zone	1	2	3	4
Actuator	F3	F3	B3	B3
Sensor at 50 mm distance	F2	F4	B2	B4
Sensor at 100 mm distance	F1	F5	B1	B5

Data processing

The voltage vs. time signal recorded for the transducers in each of the four inspection zones can be processed to obtain a range of linear and nonlinear ultrasonic parameters. Subsequently, the change in magnitude of these ultrasonic parameters with damage progression can be monitored. In the present work, two ultrasonic parameters are evaluated, namely, the Rayleigh wave velocity, c_R, and the Scaling Subtraction Method (SSM) parameter, θ. The method for determining each of these parameters is discussed briefly in the following sub-sections.

Rayleigh wave velocity, c_R. Each inspection zone has two sensors at a nominal distance of $d = 50$ mm. The Rayleigh wave velocity is calculated using the formula

$$c_R = d/\Delta t, \tag{1}$$

where Δt is the time of flight of the travelling wave, which can be evaluated using the cross-correlation technique [11]. For example, Fig. 2a shows the time-domain signals for sensors F2 and F1 in the undamaged specimen and Fig. 2b shows that variation of the cross-correlation of the two signals with the time shift in the signal of F2. The time of flight is taken as the time shift at which the cross-correlation is maximised. The Rayleigh wave velocities in the four inspection zones of the undamaged specimen are reported in Table 2. The wave velocity on the back surface of the specimen is roughly 14% greater than the front surface, possibly due to non-uniform distribution of aggregate in the specimen or due to the presence of pre-existing defects underneath the front surface. The wavelength of the Rayleigh wave at the excitation frequency (65 kHz), calculated from the velocities in Table 2, lies in the range of 32 mm to 41 mm. The wavelength is comparable to the sensor spacing of 50 mm but approximately 10 times smaller than the specimen width and depth.

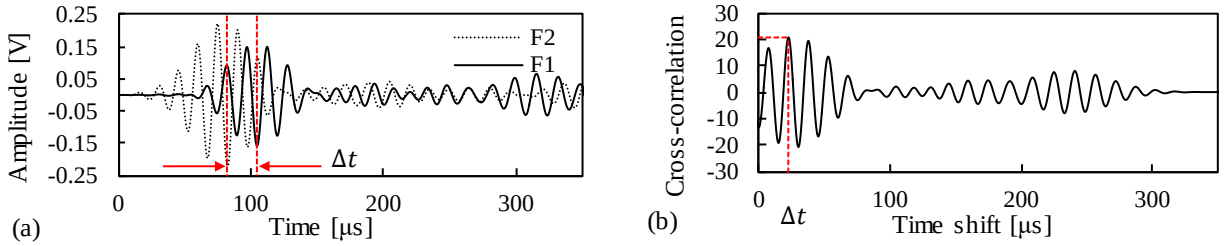

Fig. 2: (a) time domain signals of sensors F2 and F1 in zone 1, (b) cross-correlation of the two signals vs. the time shift of the signal of F2.

Table 2: Rayleigh and longitudinal wave speed calculations for undamaged specimen

Propagation path	F2 to F1	F4 to F5	B2 to B1	B4 to B5
Time of flight, Δt [μs]	22.433333	22.766666	19.233333	21.133333
Distance, d [mm]	50 ± 2	50 ± 2	50 ± 2	50 ± 2
Wave velocity, c_R [m/s]	2229 ± 89	2196 ± 88	2600 ± 104	2366 ± 95

Scaling-Subtraction Method (SSM) parameter, θ. The response of a specimen, $v_l(t)$, excited by an elastic wave of sufficiently low amplitude, $A_{o,l}$, is quasi-linear regardless of the damage state. At large excitation amplitudes, $A_o = kA_l$ $(k \gg 1)$, the specimen response, $v_{nl}(t)$, becomes nonlinear, i.e. not proportional to the excitation voltage. The residual signal, $v_{res}(t)$, defined according to [9]

$$v_{res}(t) = v_{nl}(t) - kv_l(t), \quad k = A_o/A_{o,l}, \tag{2}$$

can provide an indication of the material nonlinearity. In Eq. (2), $v_{nl}(t)$ and $v_l(t)$ are the windowed time domain signals from a sensor at high and low excitation voltages, respectively.

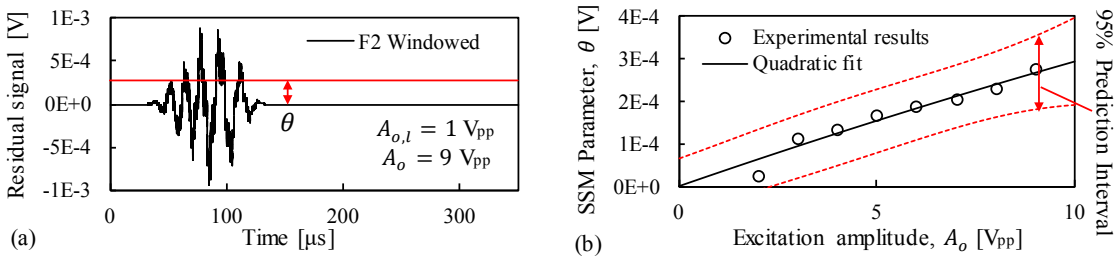

Fig. 3: (a) Example of a residual signal obtained using SSM for the undamaged specimen, (b) Baseline dependence of the SSM parameter on the excitation amplitude evaluated from sensor F2 output.

The RMS amplitude θ of the residual signal obtained from Eq. (2) can serve as a nonlinear parameter, defined as

$$\theta = \sqrt{\Sigma v_{res}^2(t_i)/n}, \quad i = 1,2,\dots,n, \tag{3}$$

where n is the number of samples in the windowed signal.

Fig. 3a shows the residual signal obtained for sensor F2 in the undamaged specimen for $\boldsymbol{k = 9}$ in Eq. (2). The signal $\boldsymbol{v_{nl}(t)}$ was obtained at an excitation voltage of 9 V_{pp} and the signal $\boldsymbol{v_l(t)}$ was obtained at an excitation voltage of 1 V_{pp}. Fig. 3b shows the experimentally obtained dependence of the nonlinear parameter $\boldsymbol{\theta}$ on the excitation amplitude $\boldsymbol{A_o}$ as well as the prediction bounds obtained through curve fitting.

Specimen loading procedure

Damage was induced in the specimen by applying a uniaxial compressive load along the longitudinal direction of the specimen using a 5000 kN hydraulic press (Fig. 4). The specimen was loaded and unloaded cyclically and the maximum load was incremented by 90 kN per cycle until failure was reached. Ultrasonic measurements were performed on the unloaded specimen at the end of each cycle. The specimen failed at a load of 2730 kN corresponding to a compressive strength of approximately 30 MPa.

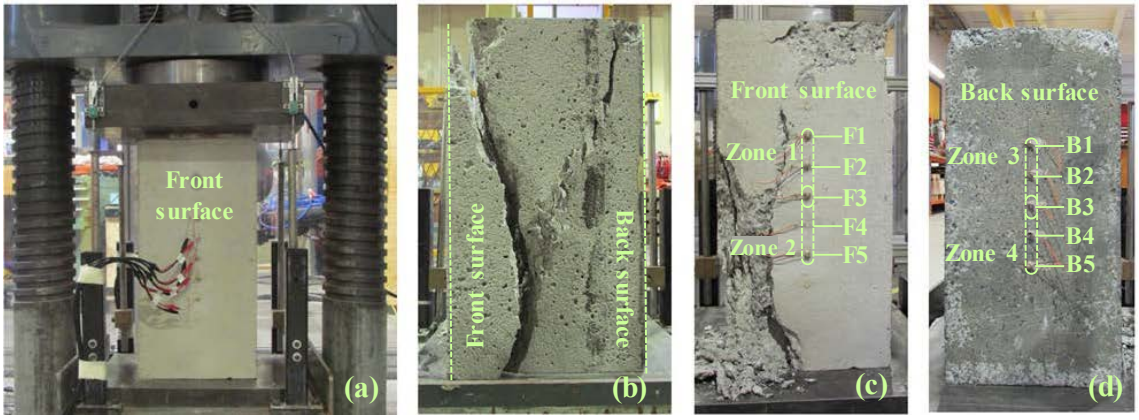

Fig. 4: (a) Arrangement of the test specimen in the hydraulic press, (b) side view of the fractured specimen, (c-d) front and back views of the fractured specimen.

Sensitivity of ultrasonic parameters to compressive damage

From Eq. (1), the relative change in Rayleigh wave velocity in the damaged specimen can be obtained as

$$\frac{\Delta c_R}{c_{R0}} = \frac{c_R - c_{R0}}{c_{R0}} = \frac{d/\Delta t - d/\Delta t_0}{d/\Delta t_0} = -\frac{(\Delta t - \Delta t_0)}{\Delta t} \tag{4}$$

where Δt_0 is the baseline value of the time of flight between two sensors in the undamaged state and Δt is the time of flight in the unloaded but damaged specimen. Fig. 5a presents the dependence of the relative change in Rayleigh wave velocity upon the normalised compressive load. The results obtained for inspection zones 1 and 2 on the front surface are in close agreement, and a similar trend is observed for inspection zones 3 and 4 on the back surface. However, the wave velocity decreases more rapidly with progressive loading on the front surface than the back surface. The maximum relative change at failure load is greater than 10% for the front surface and approximately 1% for the back surface.
The relative change in the nonlinear SSM parameter, θ with respect to its baseline value,θ_0, as shown in Fig. 5b, is over two orders of magnitude greater than the relative change in the Rayleigh wave velocity.

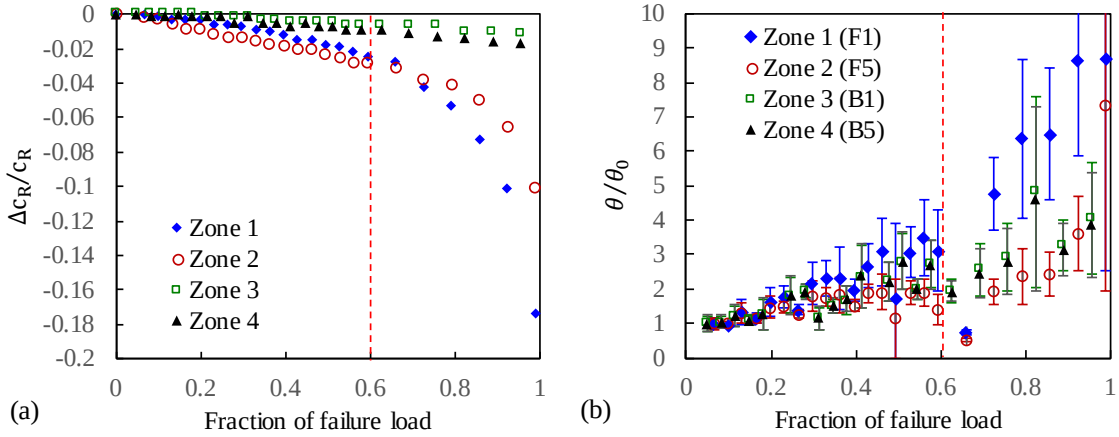

Fig. 5: (a) Relative change in Rayleigh wave velocity, and (b) Normalised SSM parameter, vs. the normalised compressive load on specimen.

Summary

The measurements for both ultrasonic parameters along the inspection zones 1 and 2 on the front surface exhibit an abrupt change in slope at approximately 60% of the failure load. This trend is not clearly observed for either parameter along the inspection zones 3 and 4 on the back surface. This observation indicates the localisation of damage near the front surface, possibly due to the presence of pre-existing defects.

References

[1] D.M. McCann, M.C. Forde, Review of NDT methods in the assessment of concrete and masonry structures, NDT E Int. 34 (2001) 71–84.

[2] H.P. Chen, Structural Health Monitoring of Large Civil Engineering Structures, John Wiley & Sons, Hoboken, 2018.

[3] J.L. Rose, Ultrasonic Waves in Solid Media, Cambridge University Press, Cambridge, 1999.

[4] S.F. Selleck, E.N. Landis, M.L. Peterson, S.P. Shah, J.D. Achenbach, Ultrasonic investigation of concrete with distributed damage, ACI Mater. J. 95 (1998), 27-36.

[5] J.O. Owino, L.J. Jacobs, Attenuation measurements in cement-based materials using laser ultrasonics. J. Eng. Mech. 125 (1999), 637-647.

[6] L.A. Ostrovsky, P.A. Johnson, Dynamic nonlinear elasticity in geomaterials. La Rivista del Nuovo Cimento 24 (2000), pp. 48.

[7] M. Meo, Nonlinear acoustic and ultrasound methods for assessing and monitoring civil infrastructures, in: M.L. Wang, J.P. Lynch, H. Sohn (Eds.), Sensor Technologies for Civil Infrastructures Vol. 1, Woodhead Publishing, Cambridge, 2014, pp. 179-200.

[8] K. Van Den Abeele, J. De Visscher, Damage assessment in reinforced concrete using spectral and temporal nonlinear vibration techniques. Cem. Concr. Res. 30 (2000), 1453-1464.

[9] P. Antonaci, C.L.E. Bruno, A.S. Gliozzi, M. Scalerandi, Monitoring evolution of compressive damage in concrete with linear and nonlinear ultrasonic methods, Cem. Concr. Res. 40 (2010), 1106-1113.

[10] H. Mohseni, C.T. Ng, Rayleigh wave propagation and scattering characteristics at debondings in fibre-reinforced polymer-retrofitted concrete structures, Struct Health Monitor. (2018), https://doi.org/10.1177/1475921718754371.

[11] D. Marioli, C. Narduzzi, C. Offelli, D. Petri, E. Sardini, A. Taroni, Digital Time-of-Flight Measurement for Ultrasonic Sensors, IEEE Trans. Instrum. Meas. 41 (1992), 93-97.